Heliyon 10 (2024) e29826

Contents lists available at ScienceDirect

Heliyon

journal homepage: www.cell.com/heliyon

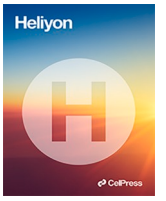

Research article

Feeding rhythm of the zoea larvae of *Scylla paramamosain*: The dynamic feeding rhythm is not completely synchronized with photoperiod

Wei Wang [1], Zhiqiang Liu [1], Xueyang Wang, Fengying Zhang, Chunyan Ma, Ming Zhao, Keyi Ma [*], Lingbo Ma [**]

Key Laboratory of East China Sea Fishery Resources Exploitation, Ministry of Agriculture and Rural Affairs, East China Sea Fisheries Research Institute, Chinese Academy of Fishery Sciences, Yangpu Area, Shanghai 200090, PR China

ARTICLE INFO

Keywords:
Scylla paramamosain
Zoea
Feeding rhythm
Feeding rate
Digestive enzyme

ABSTRACT

The feeding rhythm is one of the key factors determining the success of artificial breeding of *S. paramamosain.* To understand the feeding rhythm of the different zoea larva developmental stages of *S. paramamosain*, the feeding rate, digestive enzyme activity, and expression of metabolism-related genes were investigated in the present study. The results showed that the *S. paramamosain* feeding rate has strong diurnal feeding rhythm, being significantly higher at 10:00–14:00 from stages ZI to ZIV. While the feeding rate peaked at 14:00 on Days 10 and 11, the peak shifted to 18:00 on Day 12. The activity of digestive enzymes amylase, pepsin and lipase decreased at night but increased in the daytime, showing a single-phase rhythm similar to that of the feeding rate, suggesting that the digestive enzyme activity was closely associated with the feeding rate during the larval development. Compared to pepsin and lipase, the activity of amylase was the most consistent with feeding rate. In particular, amylase activity peaked at 18:00 on Day 12. Due to its synchronicity with feeding activity, the activity of amylase could provide a potential reference for determining the best feeding time during zoea stages in *S. paramamosain* breeding. Moreover, the relative mRNA expression of metabolism-related genes *SpCHH* and *SpFAS* at most tested points was lower from 10:00 to 14:00, but higher at 18:00 to 6:00 of the next day. On the other hand, the expression patterns of *SpHSL* and *SpTryp* were converse to those of *SpCHH* and *SpFAS*. Our findings revealed that the *S. paramamosain* zoea has an obvious feeding rhythm, and the most suitable feeding time was 10:00–18:00 depending on different stages. The feeding rhythm is a critical aspect in aquaculture, influencing a series of physiological functions in aquatic animals. This study provides insights into the feeding rhythm during the zoea development of *S. paramamosain*, making a significant contribution to optimizing feeding strategy, improving aquafeed utilization, and reducing the impact of residual feed on water environment.

* Corresponding author. East China Sea Fisheries Research Institute, Chinese Academy of Fishery Sciences, No.300 Jungong Road, Yangpu Area, Shanghai 200090, PR China.

** Corresponding author. East China Sea Fisheries Research Institute, Chinese Academy of Fishery Sciences, No.300 Jungong Road, Yangpu Area, Shanghai 200090, PR China.

E-mail addresses: kyma1632022@163.com (K. Ma), malingbo@vip.sina.com (L. Ma).

[1] Wei Wang and Zhiqiang Liu contributed equally to this work.

https://doi.org/10.1016/j.heliyon.2024.e29826
Received 5 February 2024; Received in revised form 25 March 2024; Accepted 16 April 2024
Available online 17 April 2024

1. Introduction

The mud crab (*Scylla paramamosain*) is an economically important species, which is naturally distributed along the coasts of southeast China, and is also a vital aquaculture crab for many countries around the Indian and Pacific Oceans [1–6]. In China, the total yield of *S. paramamosain* exceeded 220 thousand tons in 2022 [7]. Despite the continuous increase in output of *S. paramamosain* over the past decade, its production still cannot fully meet the requirements of the consumer market [5]. Therefore, supplying a large number of high-quality *S. paramamosain* larvae will be essential for expanding the farming potential and increasing its yield [8,9]. Until now, the obtaining of seeds for *S. paramamosain* aquaculture have still largely relied on wild-caught sources [6,10]. Due to differing growth synchronicities of the wild-caught larvae, it is challenging to ensure juvenile crabs' early developmental performance [11]. Artificial seeds could be a good solution to the problem, through provision of adequate food and stable water quality conditions.

Feeding ability of crustaceans is influenced by many factors, such as water temperature [12,13], salinity level [3,8,9] and photoperiodic variation [14,15]. Generally, water temperature is one of the primary environmental factors influencing crustacean survival, growth, and feeding [16]. It can function alone or in conjunction with other environmental conditions [17]. Salinity as an environmental factor also plays a vital role in the growth and development of cultured mud crabs [18,19]. In aquatic environments, light is one of the most important external elements, which affects mud crabs' metabolism, antioxidant capacity, growth performance, behavior and survival [11,20,21]. In its life history, *S. paramamosain* has four distinct developmental stages, of which, the zoea larva stage is the first period after individual hatching. It is the foundation stage in artificial breeding, significantly influencing the success of *S. paramamosain* aquaculture. The zoea larval phase consists of five distinct stages punctuated by molting. These stages, namely Zoea I (ZI) to Zoea V (ZV), require a large amount of energy and nutrients to meet their growth requirements. Although there have been focused studies on the effects of systematic nutrient regulation on the development of the mud crab [5,22], little information is available on the feeding rhythm of early developmental period of *S. paramamosain*, especially in the larval stage.

Usually, the feeding rhythm of animals, such as feeding frequency and feeding time, is directly relevant to the determination of feeding strategy [23,24]. Feeding frequency influences aquatic growth and plays a crucial role in regulating feed intake [25,26]. In addition, feeding time, depending on the species and diverse developmental stages, is shown to be the most significant factor in the feeding rhythm, and affects growth performance for the animals [27]. An optimized feeding strategy based on feeding rhythm not only benefits growth and metabolism of aquatic animals, but also reduces feed wastage for aquaculture management [26,28].

Feeding time is generally related to circadian rhythm, which is an important factor affecting feeding behavior. Most organisms show daily cycles of physiological and behavioral responses for their survival and development [29]. Decapods often exhibit a change in pattern of activity in the light-dark interval or evening [30,31]. For instance, *Macrobrachium rosenbergii* larvae prefer to take in food in the evening or early at night, which indicates a nocturnal feeding profile [32]. Therefore, feeding is considered as a powerful synchronizer of circadian rhythms in aquaculture [33]. Additionally, different feeding rhythms could also affect digestive enzyme activity [34], suggesting synchrony between feeding activity and enzymatic variation. Hence, the optimization of the feeding time could be designed according to enzyme activity [33].

In the present study, by direct observation, and measuring the expression of digestion enzymes and metabolism-related genes, we investigated the feeding rhythm of the five zoea stages of *S. paramamosain* in natural light conditions. The valuable data will provide a theoretical basis for determining the best feeding time in large-scale larva cultivation, and help to improve feed utilization rate, as well as reduce the cost of *S. paramamosain* aquaculture in the future.

2. Materials and methods

2.1. Preparation of the mud crab larvae and diets

The parental crabs and zoea larvae were cultured in the Ninghai Research Center of East China Sea Fisheries Research Institute, Chinese Academy of Fishery Sciences, Zhejiang Province. The broodstocks were reared in a cement pond of 0.5 m water depth. The salinity of the sea water was ~25 ‰, and the temperature was maintained at 24–26 °C by a warming-up device comprised of a double-pipe heat exchanger (Guangdong Zuncan Technology Co., LTD, China). After spawning, gravid crabs were transferred to a 500 L black bucket with the same salinity and temperature, and kept in the dark until hatching. During this period, two-thirds of volume of the sea water in the bucket was renewed every day. Among the hatchlings, the vigorous ZI larvae were selected and transferred into a 10 m^3 cement pool with natural light for the subsequent experiments. As feed for the ZI larvae, live rotifers, cultivated with complex algae and yeast, were harvested from the rotifer cultivation ponds of our research center. As the diet for Zoea II (ZII) to ZV, *Artemia* nauplii were hatched from *Artemia* cysts, which were maintained in a black hatching barrel with incandescent lamps providing light. The incubation process of the *Artemia* nauplii was under temperature of 28 °C, and salinity of 30 ‰.

2.2. Feeding trial and sample collection

The experiments on the feeding rhythm were conducted in 250-mL beaker with the numbers of ZI to ZV larvae per 100 mL sea water being 60, 52, 40, 32 and 20, respectively. Based on our production data for cost savings and preventing reduction in the survival rate of larvae, the feed density was applied as 100 live rotifer individuals per 50 mL, and 25 *Artemia* nauplii individuals per 50 mL. Six parallel feeding trials were set up. If some larvae in the experiment died, the appropriate number of individuals in the beaker would be replenished using individuals from the cement pool which were fed with the same feeding strategy. After the feeding with live rotifers or *Artemia* nauplii, the larvae at different developmental stages were sampled every 4 h, rinsed with seawater, and stored in a −80 °C

freezer (Thermo Fisher, USA) for one day for the following RNA extraction. For the digestive enzyme activity determination, it was carried out immediately after washing. The number of remaining feeds in each beaker was recorded by counting every 4 h. Meanwhile, new live rotifer and *Artemia* nauplii were re-added into the beaker to maintain the above feed density.

2.3. Digestibility analysis

A total of 100 ZI, 80 ZII, 80 Zoea III (ZIII), 40 Zoea IV (ZIV) and 20 ZV larvae were randomly selected for analysis of the activity of digestive enzymes, including amylase, lipase, and pepsin. The activity of these enzymes was quantified using the commercial detection kits of Nanjing Jiancheng Bioengineering Institute (Nanjing, China) according to the manufacturer's instructions. One unit of amylase

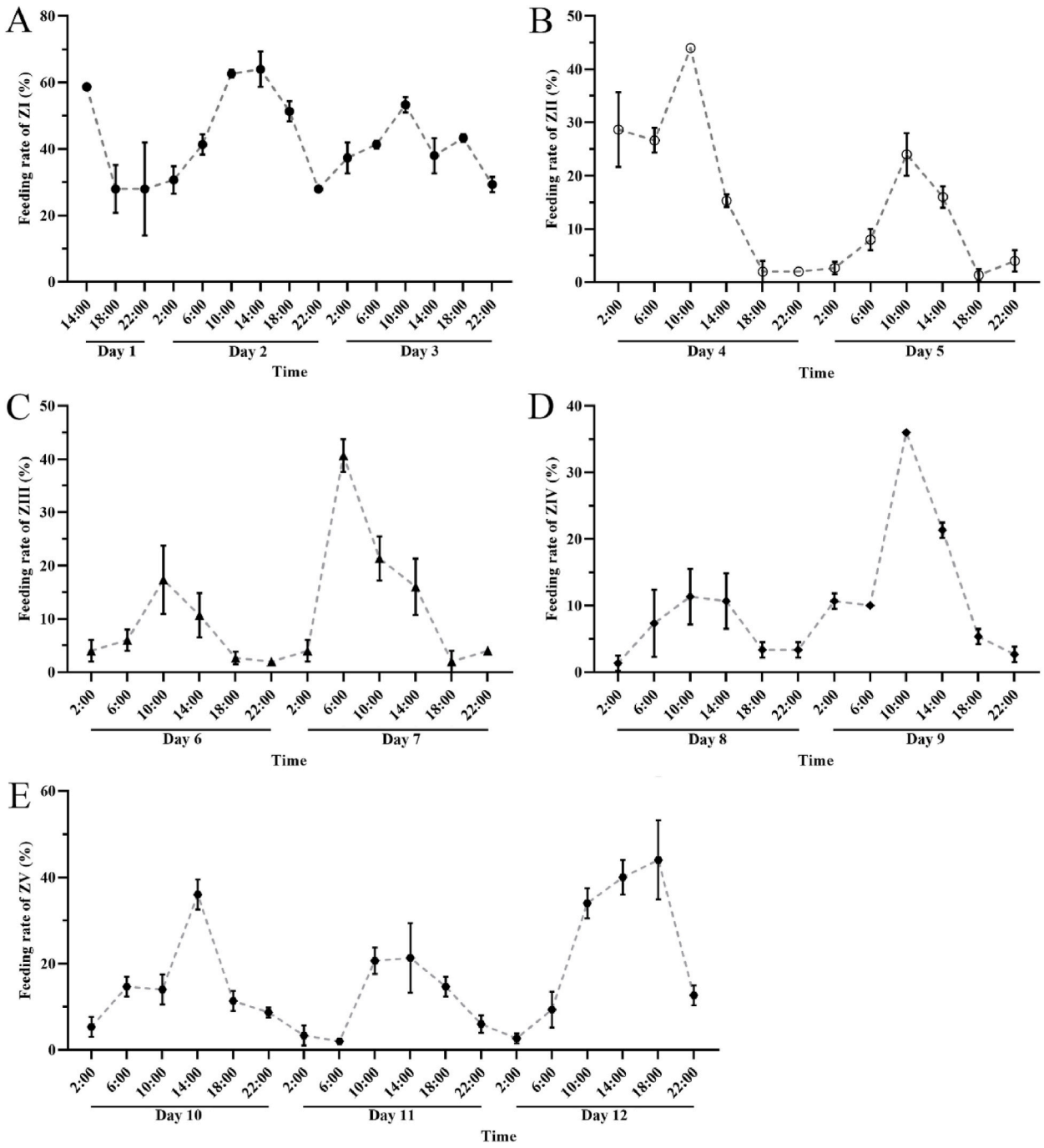

Fig. 1. Dynamic changes of feeding rate at different zoea stages in *S. paramamosain*. A: Zoea I; B: Zoea II; C: Zoea III; D: Zoea IV; E: Zoea V.

activity was defined as the hydrolysis of 10.0 mg of starch per 30 min. One unit of lipase activity was defined as 1 mmoL of substrate hydrolyzed per minute. One unit of pepsin activity was expressed as 1 mmoL of tyrosine equivalent released per minute at 37 °C [35]. Measurement for each sample was repeated three times.

2.4. RNA extraction and cDNA preparation

According to the manufacturer's instructions, total RNA from ZI to ZV were isolated by using RNAiso Plus Reagent (Takara, Japan). The number of individual samples for RNA extraction was the same as the digestibility analysis. The RNA integrity was verified based on clear bands for 18S and 28S ribosomal RNA on a 2.5 % agarose gel. RNA concentration and purity were measured using NanoDrop 2000c Spectrophotometer (Thermo, USA). Total RNA was treated with RQ1 RNase-free DNase (Promega, USA) to thoroughly remove the residual DNA. Then, the obtained RNA samples were reversely transcribed to cDNA by NovoScript® Plus All-in-one 1st Strand cDNA Synthesis SuperMix (Novoprotein, China).

2.5. Quantitative real-time PCR (qPCR)

The specific primers of metabolism-related genes for qPCR were as listed in Table S1, and qPCR was performed on an ABI 7500 system (Applied Biosystems, USA) with a 20 μL reaction mix. The real-time PCR program was as follows: 95 °C for 5 min followed by 40 cycles of 95 °C for 20 s, 60 °C for 15 s, and 72 °C for 20 s. The *18S rRNA* gene was selected as an endogenous control. A reaction without cDNA was used as the negative control. The triplicate fluorescence intensities of each sample, as measured by the crossing-point (Ct) values, were compared and converted to fold differences. The expression levels were calculated using the $2^{-\Delta\Delta CT}$ method [36].

2.6. Statistical analysis

The feeding rate was calculated using the following formula: the number of individuals of dietary intakes divided by total number of individuals of the fed live rotifers or *Artemia* nauplii. Basic statistical analysis of data was performed using SPSS 23.0, employing one-way ANOVA followed by Duncan's multiple-range test to identify significant differences. The results were expressed as mean ± standard error (SE). $P < 0.05$ was considered statistically significant, and represented by different letters.

3. Result

3.1. Feeding rates

The zoea stage of *S. paramamosain* lasted for twelve days in total, in which the ZI, ZII, ZIII, ZIV and ZV stages took up three, two, two, two and three days, respectively (Fig. 1). On Day 1, the peak of feeding rate appeared at 14:00, immediately after feeding. Then the feeding rate significantly decreased, and reached new peaks from 10:00 to 14:00 on Day 2 with the feeding rate reaching 60 % ($P < 0.05$) (Table 1). Subsequently, the feeding rate markedly decreased to a minimum at 22:00 on Day 2, which was the lowest food intake for ZI stage, with the feeding rate less than 30 %. On Day 3, the peak of the feeding rate emerged at 10:00, but fluctuated down until another minimum occurred at 22:00 (Fig. 1A). Due to the change in size of feed when converting from rotifers for ZI to *Artemia* nauplii for the following stages, the holistic feeding rates for these later stages were decreased compared with those at the ZI stage (Table 1).

At the ZII stage, the peaks of the feeding rate in both of the two days occurred at 10:00 ($P < 0.05$) (Fig. 1B). From 18:00 to 2:00, the feeding rates were quite low, especially at 18:00 on Day 5. On the other hand, at the ZIII and ZIV stages, the feeding rates during the second daytime were much higher than those during the first daytime (Fig. 1C and D). Moreover, the intakes in the evening were significantly declined compared with the daytime.

As shown in Fig. 1E, at the ZV stage, the time of feeding rate peak had changed compared with the former stages. The highest peaks of feeding rates on Days 10 and 11 were at 14:00, followed by those at 6:00 (Day 10) or 10:00 (Day 11). On Day 12, the peak had shifted

Table 1
Feeding rate during the five stages of zoea larvae.

Zoea stage	2:00	6:00	10:00	14:00	18:00	22:00
ZI (Day 1)	–	–	–	58.7 % ± 1.2%^{a}	28.0 % ± 7.2%^{b}	28.0 % ± 14.0%^{b}
ZI (Day 2)	30.7 % ± 4.2%^{d}	41.3 % ± 3.1%^{c}	62.7 % ± 1.2%^{a}	64.0 % ± 5.3%^{a}	51.3 % ± 3.1%^{b}	28.0 % ± 0.0%^{d}
ZI (Day 3)	37.3 % ± 4.6%^{b}	41.3 % ± 1.2%^{b}	53.3 % ± 2.3%^{a}	38.0 % ± 5.3%^{b}	43.3 % ± 1.2%^{b}	29.3 % ± 2.3%^{c}
ZII (Day 4)	28.7 % ± 7.0%^{b}	26.7 % ± 2.3%^{b}	44.0 % ± 0.0%^{a}	15.33 % ± 1.15%^{c}	2.0 % ± 2.0%^{d}	2.0 % ± 0.0%^{d}
ZII (Day 5)	2.7 % ± 1.2%^{d}	8.0 % ± 2.0%^{c}	24.0 % ± 4.0%^{a}	16.0 % ± 2.0%^{b}	1.3 % ± 1.2%^{d}	4.0 % ± 2.0%^{cd}
ZIII (Day 6)	4.0 % ± 2.0%^{c}	6.0 % ± 2.0%^{bc}	17.3 % ± 6.4%^{a}	10.7 % ± 4.2%^{b}	2.7 % ± 1.2%^{c}	2.0 % ± 0.0%^{c}
ZIII (Day 7)	4.0 % ± 2.0%^{c}	40.7 % ± 3.1%^{a}	21.3 % ± 4.2%^{b}	16.0 % ± 5.3%^{b}	2.0 % ± 2.0%^{c}	4.0 % ± 0.0%^{c}
ZIV (Day 8)	1.3 % ± 1.2%^{bc}	7.3 % ± 3.1%^{abc}	11.3 % ± 4.2%^{a}	10.7 % ± 4.2%^{ab}	3.3 % ± 1.2%^{bc}	3.3 % ± 1.2%^{bc}
ZIV (Day 9)	10.7 % ± 1.2%^{c}	10.0 % ± 0.0%^{c}	36.0 % ± 0.0%^{a}	21.3 % ± 1.2%^{b}	5.3 % ± 1.2%^{d}	2.7 % ± 1.2%^{d}
ZV (Day 10)	5.3 % ± 2.3%^{d}	14.7 % ± 2.3%^{b}	14.0 % ± 3.5%^{b}	36.0 % ± 3.5%^{a}	11.3 % ± 2.3%^{bc}	8.7 % ± 1.2%^{cd}
ZV (Day 11)	3.3 % ± 2.3%^{c}	2.0 % ± 0.0%^{c}	20.7 % ± 3.1%^{a}	21.3 % ± 8.1%^{a}	14.7 % ± 2.3%^{b}	6.0 % ± 2.0%^{c}
ZV (Day 12)	2.7 % ± 1.2%^{d}	9.3 % ± 4.2%^{cd}	34.0 % ± 3.5%^{b}	40.0 % ± 4.0%^{ab}	44.0 % ± 9.2%^{a}	12.7 % ± 2.3%^{c}

Note: Different superscripts in the same row indicate significant differences ($P < 0.05$) among feeding time groups.

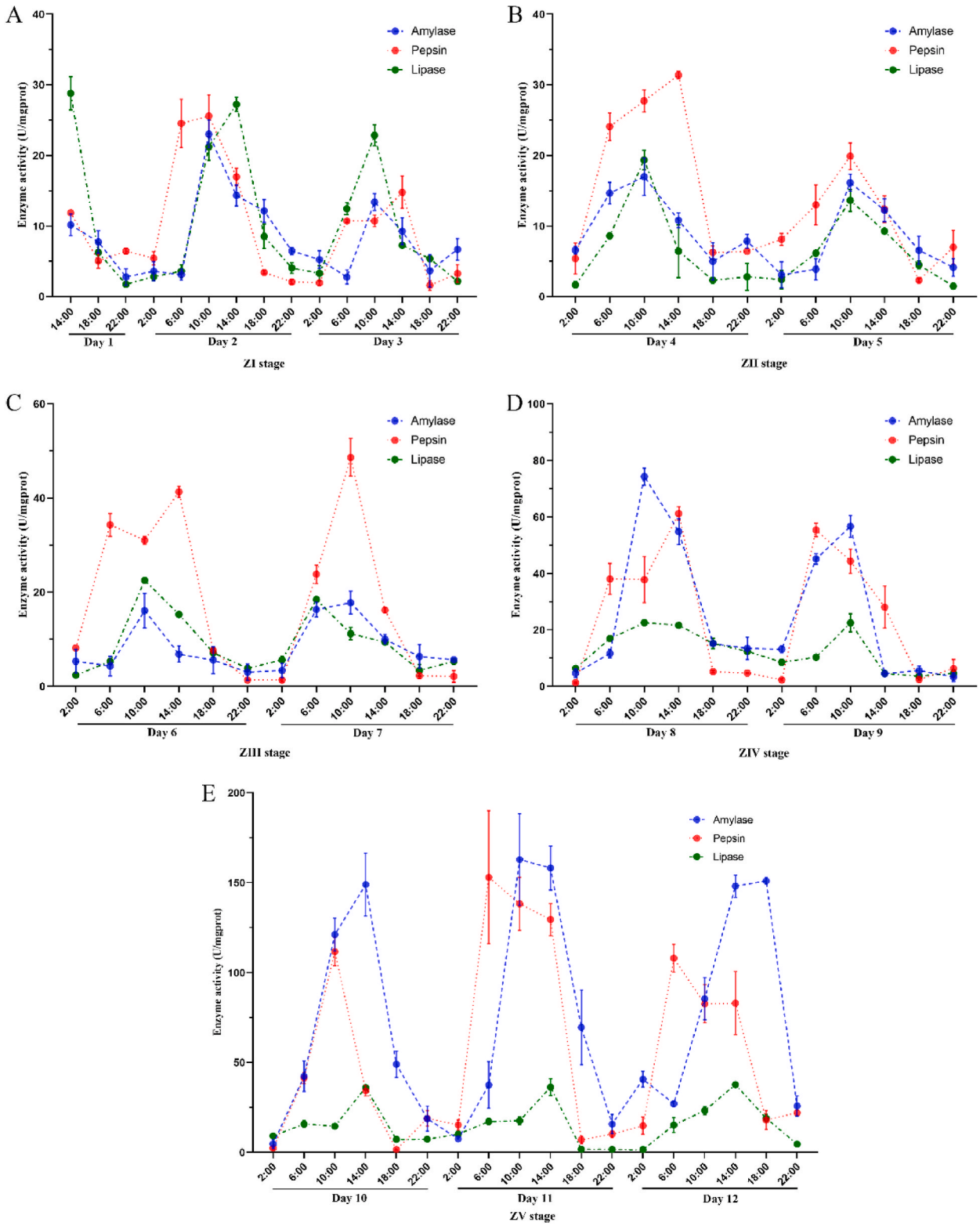

Fig. 2. Digestive enzyme activity of different zoea stages in *S. paramamosain* after food intake. A: Zoea I; B: Zoea II; C: Zoea III; D: Zoea IV; E: Zoea V.

to 18:00, with the feeding rates being significantly higher than those at 2:00, 6:00, 10:00 and 22:00 (Table 1).

3.2. Digestive enzyme activity

As shown in Fig. 2, the activity of the digestive enzymes displayed correspondence to the circadian rhythm at the five developmental stages. The first peaks of all enzyme activities occurred at 14:00 on Day 1, and then the activity gradually declined (Fig. 2A, and Table 2). For amylase and lipase, their lowest enzyme activities occurred at 22:00 on Day 1. On Day 2, the pepsin activity significantly increased at 6:00 (Fig. 2A), while the activities of amylase and lipase reached their peaks at 10:00 and 14:00, respectively. Subsequently, their activities markedly decreased, and displayed fairly low expression from 22:00 of Day 2 to 2:00 of Day 3. Thereafter, the activity of amylase continued to decline, with its lowest expression occurring at 6:00 on Day 3, while the activities of the other two enzymes began to rise when fed at 6:00 of Day 3. From the dynamic changes of enzyme activity on Day 2 and Day 3, the highest activity of the three enzymes occurred from 10:00 to 14:00.

At the ZII stage (Fig. 2B), the activity of pepsin increased from 6:00 to 14:00 after feeding on Day 4. The pepsin activity reached the highest at 14:00 and then showed a downward trend, becoming significantly different at 18:00 and 22:00 ($P < 0.05$). Then its activity increased again from 2:00 to 10:00 on Day 5, and notably peaked at 10:00 compared with the following time points. Lipase and amylase activities showed similar results, peaking at day time and reaching relatively low levels from 18:00 to 2:00. Compared to pepsin, the activities of lipase and amylase peaked at 10:00 on Day 4. The changes of pepsin and amylase activities were similar at the ZII and ZIII stages, when the peaks emerged at 14:00 on Day 6 and 10:00 on Day 7 for pepsin, and at 10:00 on Day 6 and Day 7 for amylase (Fig. 2C). In contrast, the peak of lipase activity occurred at 6:00 on Day 7.

At the ZIV stage (Fig. 2D), the pepsin and amylase activities showed an upward trend and reached the highest expression levels at 14:00 and 10:00 on Day 8, respectively ($P < 0.05$). Their activities then decreased rapidly from 18:00 to 2:00 ($P < 0.05$), which was similar to the pattern during the ZIII period. On Day 9, although the activity peaks of pepsin and amylase again occurred in daytime, the highest expression of pepsin activity became more in advance at 6:00, compared with the situation on Day 7 of ZIII. The lipase activity peaked at 10:00 on Day 8 and Day 9, and the activity change was not as dramatic as pepsin and amylase.

Throughout the three days at the ZV stage (Fig. 2E), the lipase activity displayed an upward trend from 2:00 to 14:00, and reached

Table 2
Change of digestive enzyme activity at different zoea stages (U/mgprot).

Enzyme	Zoea stage	2:00	6:00	10:00	14:00	18:00	22:00
Amylase	ZI (Day 1)	–	–	–	10.17 ± 1.52^{a}	7.75 ± 1.59^{a}	2.80 ± 1.17^{b}
	ZI (Day 2)	3.62 ± 1.35^{d}	3.12 ± 0.76^{d}	23.03 ± 1.96^{a}	14.36 ± 1.49^{b}	12.15 ± 1.62^{b}	6.48 ± 0.50^{c}
	ZI (Day 3)	5.26 ± 1.22^{cd}	2.78 ± 0.99^{d}	13.40 ± 1.18^{a}	9.27 ± 1.19^{b}	3.68 ± 2.23^{d}	6.69 ± 1.53^{bc}
	ZII (Day 4)	6.60 ± 0.53^{c}	14.67 ± 1.53^{a}	16.99 ± 2.64^{a}	10.83 ± 1.04^{b}	5.00 ± 2.65^{c}	7.87 ± 1.00^{bc}
	ZII (Day 5)	3.09 ± 1.87^{d}	3.88 ± 1.48^{cd}	16.15 ± 1.23^{a}	12.25 ± 1.65^{b}	6.57 ± 1.99^{c}	4.14 ± 1.26^{cd}
	ZIII (Day 6)	5.33 ± 2.52^{b}	4.33 ± 2.08^{b}	16.09 ± 3.69^{a}	6.85 ± 1.70^{b}	5.57 ± 2.89^{b}	3.00 ± 1.73^{b}
	ZIII (Day 7)	3.38 ± 1.51^{c}	16.33 ± 1.53^{a}	17.79 ± 2.42^{a}	10.00 ± 1.00^{b}	6.33 ± 2.52^{c}	5.67 ± 0.58^{c}
	ZIV (Day 8)	4.67 ± 1.53^{d}	11.67 ± 1.53^{c}	74.33 ± 3.06^{a}	54.79 ± 4.60^{b}	15.12 ± 0.83^{c}	13.45 ± 4.00^{c}
	ZIV (Day 9)	13.17 ± 1.26^{c}	45.16 ± 1.89^{b}	56.68 ± 3.81^{a}	4.50 ± 0.10^{d}	5.61 ± 1.62^{d}	3.34 ± 1.52^{d}
	ZV (Day 10)	4.67 ± 2.52^{d}	42.33 ± 8.39^{c}	121.11 ± 9.17^{b}	148.95 ± 17.41^{a}	48.99 ± 7.31^{c}	18.77 ± 6.93^{d}
	ZV (Day 11)	7.55 ± 0.51^{d}	37.49 ± 12.97^{c}	162.89 ± 25.51^{a}	158.17 ± 12.30^{a}	69.48 ± 20.68^{b}	15.81 ± 5.29^{cd}
	ZV (Day 12)	40.74 ± 4.44^{c}	27.07 ± 1.49^{d}	85.43 ± 11.69^{b}	148.03 ± 6.26^{a}	150.94 ± 1.84^{a}	25.82 ± 5.57^{d}
Pepsin	ZI (Day 1)	–	–	–	11.86 ± 0.45^{a}	5.06 ± 1.04^{b}	6.45 ± 0.40^{b}
	ZI (Day 2)	5.44 ± 0.96^{c}	24.52 ± 3.44^{a}	25.60 ± 2.96^{a}	16.98 ± 1.23^{b}	3.44 ± 0.24^{c}	2.10 ± 0.32^{c}
	ZI (Day 3)	1.96 ± 0.34^{c}	10.73 ± 0.18^{b}	10.73 ± 0.83^{b}	14.80 ± 2.27^{a}	1.61 ± 0.67^{c}	3.27 ± 1.26^{c}
	ZII (Day 4)	5.40 ± 2.18^{c}	24.09 ± 1.94^{b}	27.73 ± 1.56^{b}	31.40 ± 0.53^{a}	6.25 ± 0.95^{c}	6.41 ± 0.35^{c}
	ZII (Day 5)	8.12 ± 0.84^{bc}	13.01 ± 2.83^{b}	19.90 ± 1.87^{a}	12.40 ± 1.87^{b}	2.32 ± 0.26^{cd}	7.00 ± 2.38^{cd}
	ZIII (Day 6)	8.16 ± 0.01^{c}	34.33 ± 2.42^{b}	31.06 ± 0.83^{b}	41.32 ± 1.16^{a}	7.67 ± 0.20^{c}	1.37 ± 0.15^{d}
	ZIII (Day 7)	1.35 ± 0.38^{d}	23.83 ± 1.97^{b}	48.66 ± 4.00^{a}	16.20 ± 0.54^{c}	2.27 ± 0.66^{d}	2.11 ± 1.24^{d}
	ZIV (Day 8)	1.28 ± 0.28^{c}	38.08 ± 5.52^{b}	37.82 ± 8.13^{b}	61.20 ± 2.34^{a}	5.23 ± 0.42^{c}	4.74 ± 0.14^{c}
	ZIV (Day 9)	2.31 ± 0.42^{d}	55.35 ± 2.38^{a}	44.36 ± 4.32^{b}	28.09 ± 7.51^{c}	2.48 ± 0.47^{d}	6.33 ± 3.23^{d}
	ZV (Day 10)	2.37 ± 0.86^{d}	41.37 ± 3.04^{b}	111.65 ± 7.81^{a}	34.29 ± 2.85^{b}	1.47 ± 0.10^{d}	19.01 ± 4.27^{c}
	ZV (Day 11)	15.30 ± 2.83^{b}	153.01 ± 36.99^{a}	138.23 ± 14.62^{a}	129.46 ± 8.85^{a}	6.99 ± 2.08^{b}	10.23 ± 1.86^{b}
	ZV (Day 12)	14.88 ± 4.82^{c}	107.96 ± 7.76^{a}	82.66 ± 10.57^{b}	83.01 ± 17.59^{b}	18.02 ± 5.28^{c}	22.01 ± 1.53^{c}
Lipase	ZI (Day 1)	–	–	–	28.80 ± 2.38^{a}	6.25 ± 1.39^{b}	1.76 ± 0.10^{c}
	ZI (Day 2)	2.83 ± 0.60^{d}	3.62 ± 0.90^{d}	21.11 ± 1.90^{b}	27.25 ± 0.97^{a}	8.54 ± 1.74^{c}	4.05 ± 0.74^{d}
	ZI (Day 3)	3.31 ± 1.05^{d}	12.46 ± 0.88^{b}	22.85 ± 1.47^{a}	7.28 ± 0.28^{c}	5.38 ± 0.32^{cd}	2.20 ± 0.07^{d}
	ZII (Day 4)	1.67 ± 0.45^{c}	8.60 ± 0.04^{b}	19.36 ± 1.37^{a}	6.45 ± 3.76^{b}	2.32 ± 0.18^{c}	2.83 ± 1.89^{c}
	ZII (Day 5)	2.42 ± 1.30^{d}	6.16 ± 0.10^{c}	13.64 ± 1.54^{a}	9.29 ± 0.24^{b}	4.51 ± 0.53^{c}	1.49 ± 0.27^{d}
	ZIII (Day 6)	2.40 ± 0.21^{d}	5.30 ± 0.26^{cd}	22.54 ± 0.42^{a}	15.29 ± 0.12^{b}	7.14 ± 0.99^{c}	3.85 ± 0.30^{d}
	ZIII (Day 7)	5.64 ± 0.80^{d}	18.46 ± 0.20^{a}	11.20 ± 1.31^{b}	9.42 ± 0.06^{c}	3.40 ± 1.23^{d}	5.33 ± 0.12^{d}
	ZIV (Day 8)	6.43 ± 0.36^{d}	16.92 ± 1.02^{b}	22.53 ± 0.65^{a}	21.60 ± 0.29^{a}	15.20 ± 1.85^{b}	12.44 ± 0.13^{c}
	ZIV (Day 9)	8.57 ± 1.05^{b}	10.33 ± 0.11^{b}	22.49 ± 3.17^{a}	4.55 ± 0.31^{c}	3.64 ± 0.06^{c}	4.64 ± 1.20^{c}
	ZV (Day 10)	9.23 ± 0.82^{c}	15.81 ± 1.86^{b}	14.59 ± 1.00^{b}	36.06 ± 1.41^{a}	7.21 ± 1.53^{c}	7.32 ± 0.27^{c}
	ZV (Day 11)	10.23 ± 0.14^{c}	17.21 ± 1.77^{b}	17.62 ± 2.22^{b}	36.36 ± 4.72^{a}	1.69 ± 0.42^{d}	1.62 ± 0.03^{d}
	ZV (Day 12)	1.49 ± 0.37^{e}	15.28 ± 4.06^{d}	23.26 ± 2.07^{b}	37.71 ± 0.85^{a}	19.05 ± 2.23^{c}	4.52 ± 0.41^{e}

Note: Different superscripts in the same row indicate significant differences ($P < 0.05$) among feeding time groups.

the highest at 14:00, which was significantly different from the levels at 2:00, 18:00, and 22:00 ($P < 0.05$). Although the peak of pepsin activity occurred at 10:00 on Day 10, its peaks on Day 11 and Day 12 changed to 6:00, and were significantly different in levels from those at 2:00, 14:00, 18:00 and 22:00 on Day 11, and at 2:00, 10:00, 14:00, 18:00 and 22:00 on Day 12 ($P < 0.05$) (Table 2). There were also three peaks of amylase activity occurring during the ZV stage, which were at 14:00 on Day 10, 10:00 on Day 11, and 18:00 on Day 12. The amylase activity at these time points was significantly different from other time points on Day 10 ($P < 0.05$), but there were no significant differences in its activity when comparing the 10:00 and 14:00 time points on Day 11, and comparing 14:00 and 18:00 on Day 12, after feeding ($P > 0.05$) (Table 2).

3.3. Expression of metabolism-related genes

The expression profiles of metabolism-related genes, including *crustacean hyperglycemic hormone* (*SpCHH*), *hormone sensitive lipase* (*SpHSL*), *fatty acid synthetase* (*SpFAS*) and *trypsin* (*SpTryp*), showed significantly different changes during larval development (Fig. 3 and Table S2). On Day 1, *SpHSL* and *SpTryp* were most highly expressed at 14:00, but the expression decreased from 18:00 to 22:00 ($P < 0.05$). From Day 2 to Day 9, both *SpHSL* and *SpTryp* had mostly higher expression at 10:00 among the tested time points. During the ZV stage, their highest expression levels after feeding shifted to 14:00 on Day 10 and Day 11, and eventually to 18:00 on Day 12. Inversely, most of the lowest expression patterns of *SpCHH* and *SpFAS* were observed from 10:00 to 14:00 on Day 1 to Day 11. It was clear that the expression levels of *SpCHH* and *SpFAS* gradually decreased, until they reached the lowest expression at 18:00 on Day 12. Generally, the pattern for *SpCHH* and *SpFAS* was the reverse of *SpHSL* and *SpTryp*, with lower expression levels occurring from 10:00 to 14:00, and their expression significantly increasing from 18:00 to 6:00 of the next morning. One common characteristic of the four tested genes was that on Day 12, the time of most significant down/up-regulation was dynamically changed to 18:00, which was consistent with the contemporaneous shift in peak of feeding rate (Fig. 1E).

4. Discussion

In the present study, the *S. paramamosain* feeding rate from the ZI to ZIV stages was significantly higher in the daytime, especially at 10:00–14:00, than that in the evening and at night, implying that the larvae have strong diurnal feeding rhythm. Previous studies showed that the feeding peaks of some fishes, such as *Scortum barcoo* and *Epinephelus coioides* also occurred in the daytime, which suggested that the feeding times of crustaceans and fish at certain stages of development could be mutually referenced [37,38]. The *S. paramamosain* larvae immediately entered into ZI stage after hatching. Unlike fish, the *S. paramamosain* larvae did not take along yolk to provide them with nutrients, hence the feeding rate peaked after the first feeding at 14:00 on Day 1. The result suggested that the mud crab larvae should start being fed food immediately after hatching to ensure the supplement of nutrition and energy (Video

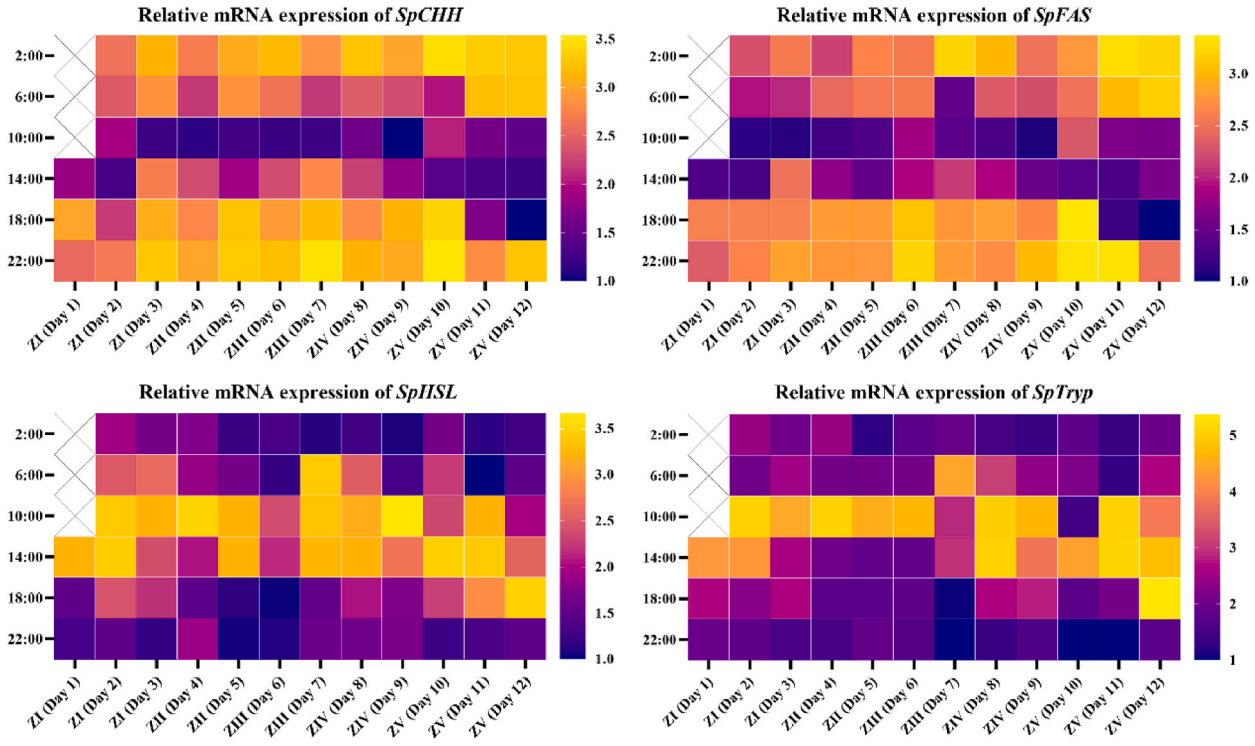

Fig. 3. Expression profiles of metabolism-related genes at *S. paramamosain* zoea stages after food intake.

S1). During the last day at the ZV stage, the time of feeding rate peak visibly shifted to 18:00. This time of feeding peak was consistent with those of megalopas and crablets during *S. paramamosain* aquaculture, and also similar to the feeding rhythm of *Eriocheir sinensis* juvenile and *Penaeus japonicus* [39,40]. The feeding rhythm is an essential aspect of aquaculture, influencing a series of physiological functions in aquatic animals [26,31,41]. Our findings revealed that rhythmic changes in feeding rate reflected the molting cycle of *S. paramamosain* zoea larvae. When the feeding peaks underwent two or three diurnal cycles with highest food intake occurring during the daytime and the lowest at night, a significant growth occurred (Fig. 1). Molting is an essential and recurring process in the growth and development of all crustaceans [5,19,42,43]. It was clear that the feeding rate of the *S. paramamosain* larvae decreased significantly before molting, and then increased again after molting was completed (the first day of the following zoea larval stage), which was similar to the change of feeding rates in *Carcinus maenas* larvae [44]. This might be due to energy consumed by the molting process. When newly formed carapace hardened, the larvae would quickly replenish lots of energy. The most suitable feeding time could be 10:00–14:00 during ZI to ZIV stages, whereas for the ZV stage, this time could be changed to 14:00–18:00. Overall, complying with the feeding strategy according to the peaks of feeding rate during the breeding of *S. paramamosain* zoea larvae would improve aquafeed utilization, save labor intensity, and reduce the pollution caused by residual feed to the water environment.

Protein, carbohydrate and lipid are three important substances in energy metabolism, and their content in the body reflects the intensity of aquatic organisms' feeding. The digestion and absorption of substances are closely related to digestive enzyme activity [45]. In our study, the activities of amylase, pepsin and lipase were found to be clearly higher from 6:00 to 14:00, or from 10:00 to 18:00 at different periods, which further confirmed that the feeding peaks occurred in the daytime.

Carbohydrate is essential to the composition and quality of aquafeed [46]. Glucose, which is completely hydrolyzed by amylase, is first absorbed by the hepatopancreas epithelial cells of crustaceans and then transported to the whole organism [47]. Therefore, the activity of amylase directly reflects the ability of crabs to decompose carbohydrates [48]. The results showed that amylase activities during the ZI, ZII and ZIII stages were lower compared with ZIV and ZV. When the larvae developed to the ZV stage, the activity of amylase increased rapidly, which could be attributed to the imperfect digestive track structure of earlier zoea stages. As the individual developed, the ability to secrete digestive enzymes became further up-regulated at the ZV stage to decompose more carbohydrates to maintain the energy expenditure caused by movement. Light is one of the most important regulators of the circadian rhythm of digestive enzyme activity [49]. Our findings revealed that the circadian rhythm of digestive enzyme activity in *S. paramamosain* larval stages was mostly related to photoperiod, showing a single-phase rhythm in one day. The current finding supports the notion that light plays an important role in digestive enzyme activity during the development of *S. paramamosain* zoea.

Compared to pepsin and lipase, the activity of amylase was the most consistent with feeding rate, especially peaking at 18:00 on Day 12. After this day, ZV individuals would metamorphose into megalopa larvae, which is one of the most essential processes influencing the success of *S. paramamosain* culture [5]. Due to the potential synchronicity of the feeding activity and enzymatic variation [50], the activity of amylase could provide a potential reference for determining the best feeding time in large-scale *S. paramamosain* larva cultivation. Adjusting feeding schedules according to variation in activity of digestive enzymes, such as amylase, could contribute to improving the production parameters of *S. paramamosain* larvae.

Crustacean hyperglycemic hormone (CHH) has important function in regulating carbohydrate metabolism in crustaceans [51], and crustaceans maintain the stability of glucose mainly through negative feedback regulation [52]. Our study showed that *SpCHH* had higher expression mainly between 18:00 and 6:00 of the next day after feeding, which was the opposite of the feeding rate, indicating that the ability of up-regulated *SpCHH* expression countered the decrease of glucose content in the hemolymph. Similarly, it has been reported that higher *SpCHH* expression could be prompted by decrease in hemolymph glucose level during the beginning of starvation [51]. Trypsin is the most abundant proteolytic enzyme, responsible for 60 % of protein digestion [53], and is thought to be associated with digestion after food intake in *S. paramamosain* [54]. The higher expression levels of *SpTryp* coincided accurately with the peaks of feeding rate. For example, both of them shifted to 18:00 on the last day during the ZV stage, suggesting the regulatory role of *SpTryp* on hydrolysis of food protein.

Lipid homeostasis involves several key processes, such as lipid uptake, fatty acid synthesis, and lipid catabolism [55]. As an important gene associated with the synthesis of long-chain fatty acids [56], *SpFAS* expression is affected by fatty acid content in diet, and can even be suppressed by polyunsaturated fatty acid (PUFA) [5]. In contrast to *SpFAS*, *SpHSL* might be involved in the process of lipolysis [57]. Fig. 3 displays the opposite expression patterns of *SpFAS* and *SpHSL* after food intake. When the feeding rates increased, *SpFAS* was notably inhibited by ingested lipids such as PUFA, resulting in a decrease in its expression. In contrast, *SpHSL* was up-regulated at these points to participate in fatty acid decomposition, implying the presence of reverse synchronous regulation of *SpFAS* and *SpHSL*. Our findings revealed that *SpFAS* and *SpHSL* could play important roles in lipid metabolism during the development of *S. paramamosain* zoea.

5. Conclusion

To our knowledge, this is the first study to elucidate the feeding rhythm during the development of the *S. paramamosain* zoea larvae. Our findings showed that the larvae generally displayed diurnal feeding rhythm, with the feeding rate and digestive enzyme activity peaking in the daytime, and declining to the lowest at night. At the ZV stage, the peak of the feeding rate and the enzyme activity of amylase and lipase was delayed in occurrence compared to the previous four phases, suggesting that the peak was dynamically changing and not completely synchronized with photoperiod. Additionally, the tested metabolism-related genes were expressed differently at the mRNA level at different times. The expression characteristics of *SpHSL* and *SpTryp* were consistent with the feeding rate, while the characteristics of *SpCHH* and *SpFAS* were the opposite. During the *S. paramamosain* zoea development, the feeding rhythm changed periodically, which was possibly related to the development period, molt cycle and light. We will pay more attention

to whether other environmental factors, such as temperature and salinity of the water environment, affect the feeding rhythm in subsequent studies.

Ethics approval

All animals were handled in accordance with guidelines established by the Animal Experiments Ethics Committee of East China Sea Fisheries Research Institute (approval number DHS-2023-1139).

Data availability statement

Data will be made available on request.

CRediT authorship contribution statement

Wei Wang: Methodology. **Zhiqiang Liu:** Writing – original draft, Software, Methodology. **Xueyang Wang:** Methodology. **Fengying Zhang:** Data curation. **Chunyan Ma:** Data curation. **Ming Zhao:** Data curation. **Keyi Ma:** Writing – review & editing, Writing – original draft, Software, Methodology. **Lingbo Ma:** Project administration, Investigation, Conceptualization.

Declaration of competing interest

The authors declare that they have no known competing financial interests or personal relationships that could have appeared to influence the work reported in this paper.

Appendix A. Supplementary data

Supplementary data to this article can be found online at https://doi.org/10.1016/j.heliyon.2024.e29826.

References

[1] L. Le Vay, V.N. Ut, M. Walton, Population ecology of the mud crab *Scylla paramamosain* (Estampador) in an estuarine mangrove system: a mark-recapture study, Mar. Biol. 151 (2007) 1127–1135, https://doi.org/10.1007/s00227-006-0553-4.
[2] H. Ye, Y. Tao, G. Wang, Q. Lin, X. Chen, S. Li, Experimental nursery culture of the mud crab *Scylla paramamosain* (Estampador) in China, Aquacult, Internat. 19 (2011) 313–321, https://doi.org/10.1007/s10499-010-9399-3.
[3] M. Niu, X. Li, Y. Chen, K. Qin, G. Liang, Y. Hu, X. Jiang, H. Wang, R. Zhu, C. Wang, C. Mu, Response of intestinal microbiota to saline-alkaline water in mud crab (*Scylla paramamosain*) based on multiple low salinity culture modes, Front. Mar. Sci. 10 (2023) 1153326, https://doi.org/10.3389/fmars.2023.1153326.
[4] H.S.A. Saqib, Y. Yuan, S.S.U.H. Kazmi, M. Tayyab, Z. Xiang, M. Ikhwanuddin, H. Ma, DNA metabarcoding reveals evidence of inter- and intra-guild predation by *Scylla paramamosain* in a marine ecosystem, Front. Mar. Sci. 10 (2023) 1206004, https://doi.org/10.3389/fmars.2023.1206004.
[5] K. Ma, Z. Liu, G. Qiao, L. Ma, F. Zhang, M. Zhao, C. Ma, W. Wang, Effects of four diets on the metabolism of megalopa metamorphosis of the mud crab, *Scylla paramamosain*, Front. Mar. Sci. 10 (2023) 1276717, https://doi.org/10.3389/fmars.2023.1276717.
[6] L. Xu, K. Ma, F. Zhang, W. Wang, L. Ma, Z. Jin, M. Zhao, W. Chen, Y. Fu, C. Ma, Z. Liu, Observations on the embryonic development of the mud crab, *Scylla paramamosain*, Front. Mar. Sci. 10 (2023) 1296509, https://doi.org/10.3389/fmars.2023.1296509.
[7] Bureau of Fisheries and Fishery Management, China Fishery Statistical Yearbook, China Agriculture Press), Beijing, China, 2023, pp. 22–58.
[8] G. Liang, K. Qin, Y. Chen, M. Niu, H. Wang, C. Wang, C. Mu, L. Chen, F. Wang, Q. Su, R. Zhu, Transcriptomic analysis of adaptive mechanisms in response to inland saline-alkaline water in the mud crab, *Scylla paramamosain*, Front. Mar. Sci. 9 (2022) 974501, https://doi.org/10.3389/fmars.2022.974501.
[9] M. Niu, G. Gao, K. Qin, Y. Chen, H. Wang, X. Li, G. Liang, C. Wang, C. Mu, Q. Su, Multiple low salinity stress modes provided novel insight into the metabolic response of *Scylla paramamosain* adapting to inland saline-alkaline water, Front. Mar. Sci. 9 (2022) 977599, https://doi.org/10.3389/fmars.2022.977599.
[10] M. Ikhwanuddin, S.S. Lan, N. Abdul Hamid, S.N. Fatihah Zakaria, M.N. Azra, A. Siti Aisah, A.B. Abol-Munafi, The embryonic development of orange mud crab, *Scylla olivacea* (Herbst, 1796) held in captivity, Iran. J. Fish. Sci. 14 (2015) 885–895.
[11] S. Chen, J. Liu, C. Shi, H. Migaud, Y. Ye, C. Song, C. Mu, Z. Ren, C. Wang, Effect of photoperiod on growth, survival, and lipid metabolism of mud crab *Scylla paramamosain* juveniles, Aquaculture 567 (2023) 739279, https://doi.org/10.1016/j.aquaculture.2023.739279.
[12] M.N. Syafaat, S. Mohammad, M.N. Azra, H. Ma, A.B. Abol-Munafi, M. Ikhwanuddin, Effect of water temperature on survival, growth and molting cycle during early crablet instar of mud crab, *Scylla paramamosain* (Estampador, 1950), Thalassas 36 (2020) 543–551, https://doi.org/10.1007/s41208-020-00233-9.
[13] M.N. Syafaat, M.N. Azra, F. Mohamad, C.Z. Che-Ismail, A. Amin-Safwan, M. Asmat-Ullah, M. Syahnon, A. Ghazali, A.B. Abol-Munafi, H. Ma, M. Ikhwanuddin, Thermal tolerance and physiological changes in mud crab, *Scylla paramamosain* crablet at different water temperatures, Animals 11 (2021) 1146, https://doi.org/10.3390/ani11041146.
[14] N. Li, J. Zhou, C. He, Y. Fu, C. Wang, L. Liu, K. Meng, Y. Li, Z. Zhu, L. Huang, D. Hu, GC-MS-based metabolomics reveal that light intensity during indoor overwintering affects the metabolism of *Scylla paramamosain*, Aquacult. Res. 52 (2021) 1013–1025, https://doi.org/10.1111/are.14956.
[15] Y. Zhang, Z. Huang, Y. Zhou, H. Ma, H.S.A. Saqib, Q. Su, W. Cui, H. Ma, The effects of different diet, salinity and light condition on growth performance and moulting cycle of juvenile mud crab, *Scylla paramamosain*, Aquacult. Res. 53 (2022) 6333–6342, https://doi.org/10.1111/are.16106.
[16] J. Gong, K. Yu, L. Shu, H. Ye, S. Li, C. Zeng, Evaluating the effects of temperature, salinity, starvation and autotomy on molting success, molting interval and expression of ecdysone receptor in early juvenile mud crabs, *Scylla paramamosain*, J. Exp. Mar. Biol. Ecol. 464 (2015) 11–17, https://doi.org/10.1016/j.jembe.2014.12.008.
[17] Q. Yuan, Q. Wang, T. Zhang, Z. Li, J. Liu, Effects of water temperature on growth, feeding and molting of juvenile Chinese mitten crab *Eriocheir sinensis*, Aquaculture 468 (2017) 169–174, https://doi.org/10.1016/j.aquaculture.2016.10.007.
[18] H.S.A. Saqib, Y. Yuan, S.S. Ul Hassan Kazmi, S. Li, H. Zheng, Y. Zhang, M. Ikhwanuddin, H. Ma, Salinity gradients drove the gut and stomach microbial assemblages of mud crabs (*Scylla paramamosain*) in marine environments, Ecol. Indic. 151 (2023) 110315, https://doi.org/10.1016/j.ecolind.2023.110315.

[19] A. Amin-Safwan, L. Gamburud, M. Izzah-Syafiah, M. Mardhiyyah, H.H. Mahsol, M. Taufik, H. Manan, M. Naimullah, C.I. Che-Zulkifli, H. Muhd-Farouk, M. N. Syafaat, M. Nadirah, H. Ma, M. Ikhwanuddin, Moulting performances evaluation of female orange mud crab, *Scylla olivacea* (Herbst, 1796) in-captivity: effects of water salinity and limb autotomy, Trop. Life Sci. Res. in press (2024), 10.21315/.

[20] X. Li, Z. Li, J. Liu, T. Zhang, C. Zhang, Effects of light intensity on molting, growth, precocity, digestive enzyme activity, and chemical composition of juvenile Chinese mitten crab *Eriocheir sinensis*, Aquacult. Int. 19 (2011) 301–311, https://doi.org/10.1007/s10499-010-9414-8.

[21] S. Chen, C. Shi, H. Migaud, C. Song, C. Mu, Y. Ye, C. Wang, Z. Ren, Light spectrum impacts on growth, molting, and oxidative stress response of the mud crab *Scylla paramamosain*, Front. Mar. Sci. 9 (2022) 840353, https://doi.org/10.3389/fmars.2022.840353.

[22] J. Luo, C. Ren, T. Zhu, C. Guo, S. Xie, Y. Zhang, Z. Yang, W. Zhao, X. Zhang, J. Lu, L. Jiao, Q. Zhou, D.R. Tocher, M. Jin, High dietary lipid level promotes low salinity adaptation in the marine euryhaline crab (*Scylla paramamosain*), Anim. Nutr. 12 (2023) 297–307, https://doi.org/10.1016/j.aninu.2022.10.004.

[23] G. Bardera, N. Usman, M. Owen, D. Pountney, K.A. Sloman, M.E. Alexander, The importance of behaviour in improving the production of shrimp in aquaculture, Rev. Aquacult. 11 (2019) 1104–1132, https://doi.org/10.1111/raq.12282.

[24] L.M. Vera, P. Negrini, C. Zagatti, E. Frigato, F.J. Sanchez-Vazquez, C. Bertolucci, Light and feeding entrainment of the molecular circadian clock in a marine teleost (*Sparus aurata*), Chronobiol. Int. 30 (2013) 649–661, https://doi.org/10.3109/07420528.2013.775143.

[25] G. Biswas, A.R. Thirunavukkarasu, J.K. Sundaray, M. Kailasam, Optimization of feeding frequency of Asian seabass (*Lates calcarifer*) fry reared in net cages under brackishwater environment, Aquaculture 305 (2010) 26–31, https://doi.org/10.1016/j.aquaculture.2010.04.002.

[26] Y. Chen, X. Wu, J. Lai, Y. Liu, M. Song, F. Li, Q. Gong, Comprehensive transcriptome analysis reveals the effect of feeding rhythm on the immunity and metabolism of *Acipenser dabryanus*, Fish Shellfish Immunol. 122 (2022) 276–287, https://doi.org/10.1016/j.fsi.2022.02.023.

[27] C. Qin, Q. Gong, Z. Wen, Y. Zou, D. Yuan, T. Shao, H. Li, Comparative analysis of the liver transcriptome of *Pelteobagrus vachellii* with an alternative feeding time, Comp. Biochem. Physiol. D: Genom. Proteonomics 22 (2017) 131–138, https://doi.org/10.1016/j.cbd.2017.04.001.

[28] S. Lee, L.Y. Haller, N.A. Fangue, J.G. Fadel, S.S.O. Hung, Effects of feeding rate on growth performance and nutrient partitioning of young-of-the-year white sturgeon (*Acipenser transmontanus*), Aquacult. Nutr. 22 (2016) 400–409, https://doi.org/10.1111/anu.12255.

[29] A. Schwarzenberger, N.H. Handke, T. Romer, A. Wacker, Geographic clines in *Daphnia magna*'s circadian clock gene expression: local adaptation to photoperiod, Zoology 144 (2021) 125856, https://doi.org/10.1016/j.zool.2020.125856.

[30] J.D. Palmer, Tidal rhythms: the clock control of the rhythmic physiology of marine organisms, Biol. Rev. 48 (1973) 377–418, https://doi.org/10.1111/j.1469-185X.1973.tb01008.x.

[31] J. Reis, A. Weldon, P. Ito, W. Stites, M. Rhodes, D.A. Davis, Automated feeding systems for shrimp: effects of feeding schedules and passive feedback feeding systems, Aquaculture 541 (2021) 736800, https://doi.org/10.1016/j.aquaculture.2021.736800.

[32] M.A. Borges de Aviz, F.A. Abrunhosa, M. Maciel, C.R. Maciel, On feeding of the freshwater prawn larvae *Macrobrachium rosenbergii*, Bol. Inst. Pesca 44 (2018) e373, https://doi.org/10.20950/1678-2305.2018.44.4.373.

[33] A.D.A. Santos, J. Fernando Lopez-Olmeda, F. Javier Sanchez-Vazquez, R. Fortes-Silva, Synchronization to light and mealtime of the circadian rhythms of self-feeding behavior and locomotor activity of white shrimps (*Litopenaeus vannamei*), Comp. Biochem. Physiol. A: Mol. Integr. Physiol. 199 (2016) 54–61, https://doi.org/10.1016/j.cbpa.2016.05.001.

[34] E. Calixto da Silva, F.C. Sterzelecki, L. Alves Musialak, J.K. Sugai, J.d.J.P. Castro, F.S. Pedrotti, C. Magnotti, F.d.S. Cipriano, V.R. Cerqueira, Effect of feeding frequency on growth performance, blood metabolites, proximate composition and digestive enzymes of Lebranche mullet (*Mugil liza*) Juveniles, Aquacult. Res. 51 (2020) 1162–1169, https://doi.org/10.1111/are.14466.

[35] Y. Zhuang, H. Huang, X.-L. Liu, N.-A. Wang, G.-F. Zhong, Effect of bovine lactoferricin on the growth performance, digestive capacity, immune responses and disease resistance in Pacific white shrimp, *Penaeus vannamei*, Fish Shellfish Immunol. 123 (2022) 282–289, https://doi.org/10.1016/j.fsi.2022.03.012.

[36] Z. Guo, J. Zuo, X. Liu, J. Gong, K. Ma, J. Feng, J. Li, S. Zhang, G. Qiu, Effects of titanium dioxide (TiO_2)/activated carbon (AC) nanoparticle on the growth and immunity of the giant freshwater prawn, *Macrobrachium rosenbergii*: potential toxicological risks to the aquatic crustaceans, Environ. Sci. Pollut. Res. 30 (2023) 33322–33333, https://doi.org/10.1007/s11356-022-24555-8.

[37] Y.S. Sun, X.Q. Zhang, D.J. Shi, X.J. Sun, D. Wei, Y.J. Liang, Feeding rhythm and daily food intake of Jade Perch *Scortum barcoo*, Fish. Sci. 31 (2012) 28–31, https://doi.org/10.3969/j.issn.1003-1111.2012.01.006 (in Chinese).

[38] H.F. Zhang, X.C. Liu, H.R. Lin, Y.Z. Liufu, Y.X. Wang, G.G. Huang, H.D. Wang, C.H. Ou, Studies on feeding rhythm and daily feeding amount of larval *Epinephelus coioides*, J. Fish. China 28 (2004) 669–674 (in Chinese).

[39] E.T. Jia, M.J. Yan, Q.C. Lai, W.T. Luo, G.Z. Jiang, W.B. Liu, D.D. Zhang, Feeding rhythm of the Chinese mitten crab (*Eriocheir sinensis*), J. Fish. Sci. China 25 (2018) 546–554, https://doi.org/10.3724/SP.J.1118.2018.17444 (in Chinese).

[40] H. Reymond, J.P. Lagardère, Feeding rhythms and food of *Penaeus japonicus* Bate (Crustacea, Penaeidae) in salt marsh ponds; role of halophilic entomofauna, Aquaculture 84 (1990) 125–143, https://doi.org/10.1016/0044-8486(90)90343-L.

[41] Y. Xu, B. Zhang, C. Yu, Z. Hung, N. Hu, Y. Cai, Y. Li, Comparative transcriptome analysis reveals the effects of different feeding times on the hepatopancreas of Chinese mitten crabs, Chronobiol. Int. 40 (2023) 569–580, https://doi.org/10.1080/07420528.2023.2189481.

[42] B. Xu, D. Tu, M. Yan, M. Shu, Q. Shao, Molecular characterization of a cDNA encoding $Na^+/K^+/2Cl^-$ cotransporter in the gill of mud crab (*Scylla paramamosain*) during the molt cycle: implication of its function in osmoregulation, Comp. Biochem. Physiol. A: Mol. Integr. Physiol. 203 (2017) 115–125, https://doi.org/10.1016/j.cbpa.2016.08.019.

[43] M. Ikhwanuddin, A.B. Abol-Munafi, M.N. Azra, Data on the molting duration and time of hardening of instar crab at different culture temperatures, Data Brief 25 (2019) 104196, https://doi.org/10.1016/j.dib.2019.104196.

[44] R.R. Dawirs, A. Dietrich, Temperature and laboratory feeding rates in *Carcinus maenas* L. (Decapoda: portunidae) larvae from hatching through metamorphosis, J. Exp. Mar. Biol. Ecol. 99 (1986) 134–147, https://doi.org/10.1016/0022-0981(86)90233-9.

[45] K.M. Das, S.D. Tripathi, Studies on the digestive enzymes of grass carp, *Ctenopharyngodon idella*, Aquaculture 92 (1991) 21–32, https://doi.org/10.1016/0044-8486(91)90005-R.

[46] Q. Zhan, T. Han, X. Li, J. Wang, Y. Yang, X. Yu, P. Zheng, T. Liu, H. Xu, C. Wang, Effects of dietary carbohydrate levels on growth, body composition, and gene expression of key enzymes involved in hepatopancreas metabolism in mud crab *Scylla paramamosain*, Aquaculture 529 (2020) 735638, https://doi.org/10.1016/j.aquaculture.2020.735638.

[47] X. Wang, E. Li, L. Chen, A review of carbohydrate nutrition and metabolism in Crustaceans, North Am. J. Aquacult. 78 (2016) 178–187, https://doi.org/10.1080/15222055.2016.1141129.

[48] X. Zhang, C. Huang, C. Guo, S. Xie, J. Luo, T. Zhu, Y. Ye, M. Jin, Q. Zhou, Effect of dietary carbohydrate sources on the growth, glucose metabolism and insulin pathway for swimming crab, *Portunus trituberculatus*, Aquaculture Reports 21 (2021) 100967, https://doi.org/10.1016/j.aqrep.2021.100967.

[49] A. Van Wormhoudt, Activités enzymatiques digestives chez Palaemon serratus: Variations annuelles de l'acrophase des rythmes circadiens, Biochem. Syst. Ecol. 5 (1977) 301–307, https://doi.org/10.1016/0305-1978(77)90030-8.

[50] D. Espinosa-Chaurand, O. Carrillo-Farnes, F. Vega-Villasante, H. Nolasco-Soria, Effect of protein level in diet and feeding schedule on the digestive enzymatic activity of *Macrobrachium tenellum* juveniles, Lat. Am. J. Aquat. Res. 47 (2019) 743–752, https://doi.org/10.3856/vol47-issue5-fulltext-3.

[51] A. Liu, J. Liu, X. Chen, B. Lu, C. Zeng, H. Ye, A novel crustacean hyperglycemic hormone (CHH) from the mud crab *Scylla paramamosain* regulating carbohydrate metabolism, Comp. Biochem. Physiol. A: Mol. Integr. Physiol. 231 (2019) 49–55, https://doi.org/10.1016/j.cbpa.2019.01.015.

[52] S. Morris, U. Postel, Mrinalini, L.M. Turner, J. Palmer, S.G. Webster, The adaptive significance of crustacean hyperglycaemic hormone (CHH) in daily and seasonal migratory activities of the Christmas Island red crab *Gecarcoidea natalis*, J. Exp. Biol. 213 (2010) 3062–3073, https://doi.org/10.1242/jeb.045153.

[53] A. Muhlia-Almazan, F.L. Garcia-Carreno, J.A. Sanchez-Paz, G. Yepiz-Plascencia, A.B. Peregrino-Uriarte, Effects of dietary protein on the activity and mRNA level of trypsin in the midgut gland of the white shrimp *Penaeus vannamei*, Comp. Biochem. Physiol. B Biochem. Mol. Biol. 135 (2003) 373–383, https://doi.org/10.1016/s1096-4959(03)00091-5.

[54] K.J. Jiang, F.Y. Zhang, D. Zhang, Q.C. Tao, Y. Zhang, Y. Pi, Z.G. Qiao, L.B. Ma, Identification of a trypsin gene from *Scylla paramamosain* and its expression profiling during larval development, Afr. J. Agric. Res. 6 (2011) 6613–6621, https://doi.org/10.5897/AJAR11.784.

[55] Y.C. Kao, P.C. Ho, Y.K. Tu, I.M. Jou, K.J. Tsai, Lipids and alzheimer's disease, Int. J. Mol. Sci. 21 (2020) 1505, https://doi.org/10.3390/ijms21041505.
[56] S.S. Chirala, S.J. Wakil, Structure and function of animal fatty acid synthase, Lipids 39 (2004) 1045–1053, https://doi.org/10.1007/s11745-004-1329-9.
[57] A.P.L. Jensen-Urstad, C.F. Semenkovich, Fatty acid synthase and liver triglyceride metabolism: housekeeper or messenger? Biochim. Biophys. Acta: Mol. Cell Biol. Lipids 1821 (2012) 747–753, https://doi.org/10.1016/j.bbalip.2011.09.017.